Fickian and Non-Fickian Sorption Kinetics of Toluene in Glassy Polystyrene

Kai-Martin Krüger and Gabriele Sadowski*

Lehrstuhl für Thermodynamik, Universität Dortmund, Emil-Figge-Str. 70, 44227 Dortmund, Germany

Received February 18, 2005; Revised Manuscript Received July 19, 2005

ABSTRACT: A gravimetric sorption apparatus is set up to measure solubilities and diffusivities in polymer−solvent systems, especially designed for measurements at low pressures and in glassy polymers. Interval sorption experiments are performed for the system toluene−polystyrene (PS) above and below the glass transition. Sorption isotherms (VLE) are obtained and diffusion coefficients are calculated in the Fickian diffusion region. Below the glass transition, non-Fickian sorption kinetics (sigmoid, two-stage) are observed.

Introduction

Solubilities and diffusivities in polymer−solvent systems are important for a number of industrial applications. In the polymer production and processing those quantities are determining the time and efficiency of the production process. In membrane separation with dense polymeric membranes, the differences in the solubilities and diffusivities of the species are essential for the separation performance. Food packaging or beverage containers are designed to prohibit the diffusion of water or gases through the polymeric barrier. In all these applications the polymer stays in rubbery/melt or the glassy state.

Other applications are coatings, membrane production, or wet fiber spinning. In those cases the polymer changes its state from rubbery to glassy through evaporation of the solvent. Here, the solubilities and the diffusivities in the rubbery as well as in the glassy state of the polymer are of interest.

There are a number of methods to measure both solubilities and diffusion coefficients in those systems. Pressure decay methods are mostly used at moderate and high pressures.[1−5] Inverse-gas chromatography, first only applied in the infinite dilution region,[6,7] has been extended by Danner and co-workers to be used in the finite concentration region as well.[8] Using a model, the solubility and diffusivities are determined from the elusion profiles. The gravimetric sorption method is the classical method, where either a quartz spring,[9−11] an electrobalance,[12,13] a quartz crystal,[14] or a magnetic suspension balance[15−18] is used to measure the weight increase or decrease of a polymer sample in a vapor atmosphere. Permeation experiments[19−21] are also capable of measuring permeabilities and diffusivities from the time lag in the steady state; the solubility can be calculated afterward from those quantities. The permeation experiments are mostly used to study gas−polymer systems. Furthermore, some spectroscopic methods are applied to determine the mass transport in such systems: FTIR-ATR,[18,22,23] forced Rayleigh scattering,[24] Rutherford backscattering,[25,26] or NMR spectroscopy.[27]

Therefore, a number of experiments exist which are applied to determine solubilities and transport kinetics in polymers. In particular, it is no problem to measure solubilities and to derive diffusion coefficients of vapors in polymers which are in the rubbery state. One can use a simple Fickian diffusion model with a temperature- and concentration-dependent diffusion coefficient to determine the diffusion coefficient from the experiments. If one intends to measure them for glassy polymers, one has to keep in mind that the glassy structure is a nonequilibrium one and that the polymer chains slowly relax. The measured quantities in the glassy region are therefore often difficult to interpret. Sometimes, in the case of nonswelling vapors a Fickian diffusion model is still appropriate to describe the diffusion behavior.[28,29] Often, the dual-mode sorption model is used for the description of sorption and diffusion of gases in glassy polymers.[1,30−32] Concerning the determination of diffusion coefficients, the situation becomes even worse if the polymer reaches its glass−rubber transition. Here, the time scale of the polymer relaxation is on the order of the diffusion time scale, and the relaxation of the polymer molecules influences the mass transport in the polymer matrix.[33,34] A simple deduction of diffusion coefficients from experiments in this region is therefore not possible anymore (maybe with the exception of a well-separated two-stage sorption behavior). This is clearly seen from the shape of the sorption curves obtained from gravimetric sorption measurements. The diffusion behavior in this case is called anomalous or non-Fickian diffusion.[35,36]

A lot of work has been done to measure solubilities and diffusivities in rubbery polymers and polymer melts[10,20,37−39] using one of the aforementioned methods. There are also numerous data on solubilities and diffusivities of simple gases,[40,41] mostly measured by permeation techniques. To determine solubilities and the mass transport in the transition region, classical sorption measurements are applied.[9,11,13,42,43]

In this work, the gravimetric sorption measurement was chosen to investigate the vapor−liquid equilibrium and the transport kinetics in glassy and rubbery polystyrene. It is applicable from the rubbery to the glassy polymer state, it is very accurate at low pressures, and if the swelling is properly taken into account, it is also extendable to higher pressures. Different shapes of polymer samples can be investigated according to the desired application or experimental time. In the case of glassy polymers thin films are preferred. Nevertheless, measuring at low pressures (just a few mbar) in

* To whom correspondence should be addressed. E-mail: G.Sadowski@bci.uni-dortmund.de.

10.1021/ma050353o CCC: $30.25
Published on Web 08/27/2005

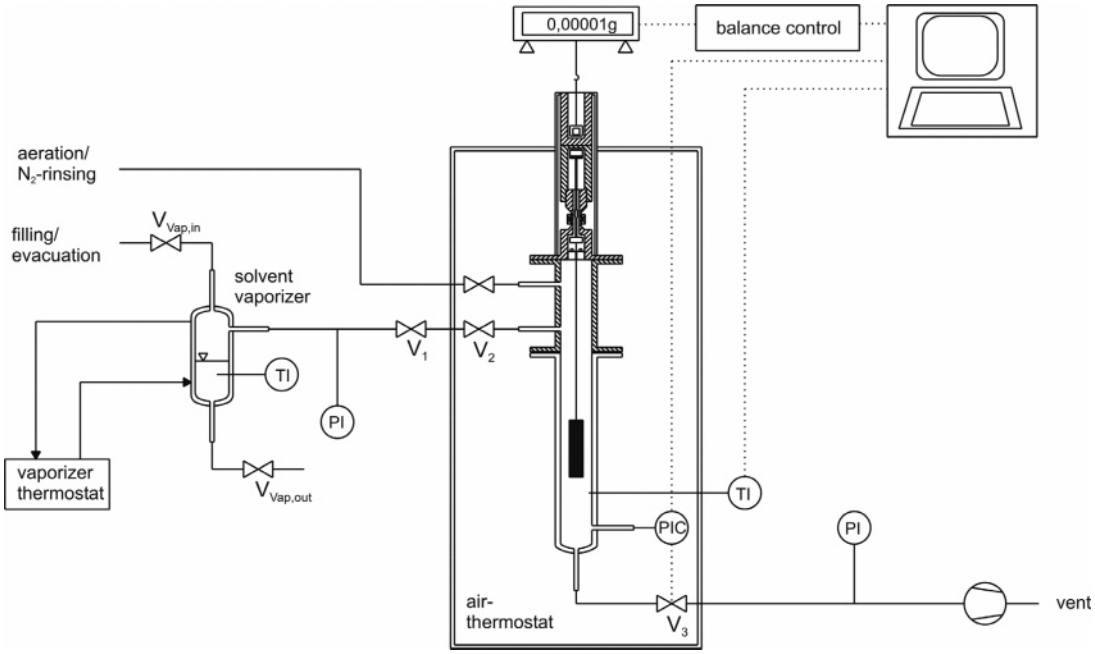

Figure 1. Flow sheet of the sorption apparatus.

glassy polymers, longer experimental times (up to several weeks) are sometimes necessary, and the problem of inevitable leakage into the equipment has to be addressed. Otherwise, there would be a severe uncertainty in the validity of the data.

For the experiments the system amorphous PS−toluene was chosen because no kinetic sorption experiments are available in the literature so far. It exists only very limited VLE data below the glass transition of the PS−toluene mixture.[63−68] In those investigations, the data below the glass transition are either very few,[63,64,66] are scattering very much,[63] are far of compared with other data,[65] or are measured using a quartz crystal microbalance.[68] The latter uses very thin polymer films and has the advantage of being rather fast, but it is thus not able to capture the slow change in the sorption equilibrium which is caused by the relaxation of the polymer matrix because this relaxation is independent of the film thickness.[53]

In the next paragraph the experimental setup will be introduced followed by the description of the experimental procedure of the sorption measurements. Afterward, experimental results for the system PS−toluene are shown and discussed with respect to Fickian and non-Fickian kinetics.

Experimental Section

Experimental Setup. To cope with the above-mentioned difficulties in experimental conditions, a gravimetric sorption equipment in a "flow-through" design was set up, which is illustrated in Figure 1.

The central device of this equipment is a magnetic suspension balance (Rubotherm),[15] measuring the weight of the sample with a reproducibility of ±0.03 mg. The weight of the sample can range from 0.01 to 30 g. The advantages of this balance are the high accuracy and long-time stability due to the balance being outside the measuring cell and having no contact to any solvent vapor. Furthermore, a continuous data readout via PC is possible, without any personnel being present during the whole time of the experiment.

The polymer sample is either hanging as a free film at the measuring hook or lying horizontally attached to the bottom of a glass bucket.

Pure solvent vapor is fed to the measuring cell from a solvent vaporizer via an inlet valve (V2) to establish a constant vapor flow through the cell. The flow is on the order of 0.1 (mbar L)/s to not affect the accuracy of the weight measurement but to be still at least 3 orders of magnitude higher than the leakage rate. Any air entering the measuring cell or the solvent vaporizer is therefore effectively removed from the equipment. An outlet control valve (V3) (MKS Type 248A) at the lower end of the cell keeps the pressure around the sample constant. The pressure in the cell is measured using a capacitive pressure transducer (MKS Baratron Type 621C) which is kept at a constant temperature of 150 °C. Thus, there is no condensation in the pressure transducer, and the temperature dependence of the transducer accuracy is avoided, resulting in an accuracy for the pressure measurement of ±0.5% of the reading. This is especially important in the low-pressure range, where solubilities of solvents in glassy polymers are of interest. The pressure in the cell can be kept constant better than ±0.1 mbar between 0.1 and 1330 mbar.

The temperature of the cell is controlled by means of an air thermostat bath, which has heating and cooling devices to keep the temperature constant to better than ±0.05 K between 20 and 150 °C. An air thermostat has the advantage that parts of the cell can easily be connected and disconnected and small temperature fluctuations in the air do not immediately influence the solvent temperature in the cell due to a low heat-transfer coefficient. The temperature in the double-walled solvent vaporizer is controlled by means of a conventional liquid thermostat. Temperatures in the vaporizer and the cell, directly below the sample, are measured using calibrated PT100 with an accuracy of ±0.05 K.

The cell and the vaporizer can each be evacuated via two connections to a vacuum pump. A computer records cell temperature, pressure, and the weight of the sample automatically.

Materials. Polystyrene was obtained from Gefinex with M_w = 280 000 g/mol and M_w/M_n = 2.94. The glass-transition temperature, obtained from DSC measurements, was about T_g = 105 °C. Poly(dimethylsiloxane) (PDMS) was obtained from GE Bayer Silicones with M_w = 60 000 g/mol and M_w/M_n ~ 3. Toluene and *n*-pentane were obtained from Merck with a purity better than 99.9% and 99.5%, respectively, and were further degassed by three successive freezing−evacuation−melting steps before being filled into the solvent vaporizer.

Film Preparation. The polymer films of thicknesses between 20 and 100 μm were prepared by casting from 23 to

60 mass % toluene solutions on a glass surface with subsequent flattening by means of a four-sided applicator exhibiting a slit of defined height (200, 500 μm) between glass and applicator surface. Desired film thicknesses could be obtained by varying solution concentration and slit height. The films were then put into a vacuum oven, and a small constant stream of air was applied to slowly remove the evaporating toluene from the polymer. After 48 h the temperature of the oven was raised to 120 °C, above the glass-transition temperature of the pure PS, to enhance the toluene removal from the film. After another 48 h vacuum was applied in order to remove the last solvent from the films. To obtain annealed films of reproducible quality, the oven was switched off after 24 h, and the film traversed the glass transition with temperature decreasing by 0.43 °C/min.

After removing from the oven, the films were immersed in warm water and easily detached from the glass surface. Pieces in the size of 25 × 90 mm or 18 × 18 mm were cut from the raw films. The latter size was used to fit the film into the bottom of the small glass bucket, in case measurements far above the glass transition where performed (110 °C). In this case the 18 × 18 mm sheet was laid onto the bottom of the glass bucket and heated to 120 °C in the oven under vacuum a second time. After 2 h at those conditions, the oven was switched off again to obtain the same cooling rate as before. Doing this, the film attached itself again to the glass. Thus, the sorption experiment was carried out as a diffusion from one side into the film. All films exhibited a thickness variation of no more than ±1.5 μm over the whole film measured by QuaNix1200 (accuracy ±1 μm + 2% Rdg).

No traces of toluene could be found in the films neither by IR spectroscopy nor by any weight decrease of the films observed under vacuum in the sorption equipment for several days.

For the PDMS measurements a glass bucket was used as well. PDMS was degassed in the sorption equipment directly, prior to the measurement.

Experimental Procedure. For the measurement of a specific isotherm and the corresponding sorption curves, two experiments are necessary. One is the actual sorption measurement, and the second is exactly the same experiment without the sample. This is done to correct for buoyancy and solvent adsorption effects on the suspension magnet and any inner parts of the magnetic coupling which are lifted together with the sample. Both experiments are performed identically as interval sorption runs.

After heating and evacuation of the system, the vaporizer is filled and subsequently heated to 1 K below the cell temperature to avoid condensation in the piping and the valves to the cell. After being sure that no solvent is present in the polymer sample from the film preparation (constant weight for at least 3 days), the pressure in the cell is stepwise increased. For this, the outlet valve V3 is closed and the inlet valves V1 and V2 are opened. If the set-point pressure is reached, the inlet valve V2 is set back to a position where the desired flow (see above) is achieved and the pressure control is set back into operation. Pressure steps could therefore be established within less than 20 or 30 s for small (<10 mbar) or large pressure steps (>10 mbar), respectively. The next pressure step followed when there was no visible weight increase for 4 days during sorption measurements. For the preceding measurement without sample, the next pressure step followed after 20−30 min.

For long runs, the vaporizer had to be refilled. In this case at the end of a sorption run, where there was basically no change in the mass of the sample, the cell was isolated by closing inlet valve V1 and outlet valve V3; the vaporizer was evacuated and refilled again. Finally, V1 and V3 were opened again, and the pressure control was switched on again. During this procedure (30−40 min) no changes in mass of the sample or in cell pressure were observed. This clearly was an experimental proof during each experiment: neither did the constant vapor stream effect the weight measurement by the balance nor was there a substantial leak into the measuring cell.

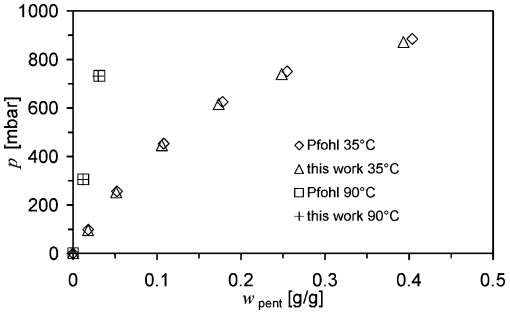

Figure 2. Experimental VLE data (vapor pressure as a function of solvent weight fraction) for *n*-pentane−PDMS for 35 and 90 °C.

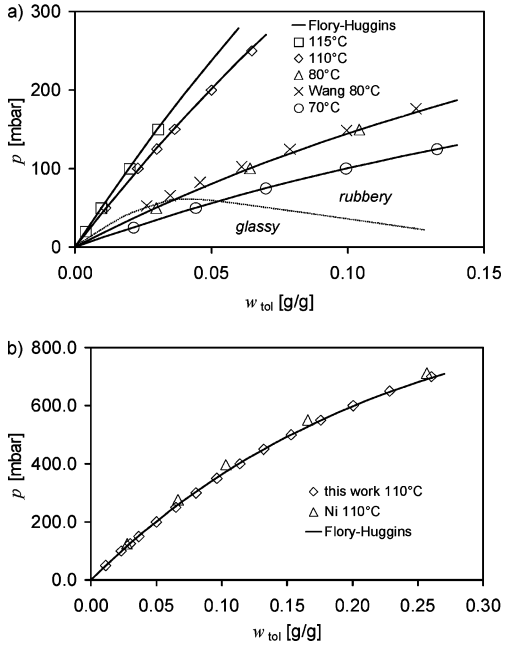

Figure 3. Experimental VLE data (vapor pressure as a function of solvent weight fraction) for toluene−PS at (a) 115, 110, 80, and 70 °C; (b) 110 °C and comparison with data from Wang[68] and Ni.[44]

Results and Discussion

Vapor−Liquid−Equilibria (VLE). The first measurements were performed with the system *n*-pentane−PDMS to check for the proper working of the equipment. Exactly the same polymer was chosen for these measurements as Pfohl et al. used in their investigation.[5] The comparison of the VLE data at 35 and 90 °C (Figure 2) shows complete agreement of the data measured by Pfohl et al. using the pressure decay method and the data measured in this work.

Having been assured that accurate data are measured with the new equipment, new data were measured for the system toluene−PS. Figure 3 shows the VLE data measured at 115, 110, 80, and 70 °C.

The shape of the sorption isotherms in Figure 3 clearly shows the well-known behavior for polymer−solvent VLE above the glass transition in a rubbery polymer condition. The bubble-point curve is a monotonically increasing function of the solvent weight fraction, the second derivative always being negative and the whole curve thus being concave to the weight-fraction axis. Although the first point of the 80 °C

isotherm and the first two of the 70 °C isotherm lie presumably below the glass transition, the shape of the isotherms seems not influenced.

Comparison with literature data (Figure 3) shows that the solubilities are slightly higher than the available literature data. This might be due to the fact that the polystyrene used in this work is a commercial product and not identical with the samples used by Ni[44] and Wang.[68]

To distinguish whether the polymer is in the rubbery state or still in the glassy state, the concentration dependence of the glass-transition temperature was estimated using a formula derived by Kelly and Bueche:[45]

$$T_g = \frac{4.8 \times 10^{-4}(1-\phi_1)T_{g1} + \alpha_S \phi_1 T_{g2}}{4.8 \times 10^{-4}(1-\phi_1) + \alpha_S \phi_1} \quad (1)$$

T_{g1} and T_{g2} are the glass-transition temperatures of the solvent and the pure polymer, respectively. α_S is the thermal expansion coefficient of the pure solvent, and ϕ_1 is the solvent volume fraction, which under the assumption of no excess volume is related to the solvent weight fraction w_1 as follows:

$$w_1 = \frac{{v_{01}}^{-1}(T,p)\phi_1}{{v_{02}}^{-1}(T,p) + \phi_1({v_{01}}^{-1}(T,p) - {v_{02}}^{-1}(T,p))} \quad (2)$$

v_{01} and v_{02} are the specific volumes of the solvent and the polymer, respectively. They are calculated at the pressure p and temperature T of the mixture using an empirical correlation[46] for v_{01} in cm^3/g:

$$v_{01}(T) = \frac{1000/M_1}{A/B^{[1+(1-T/C)^D]}} \quad (3)$$

and the Tait equation[47] for v_{02} in cm^3/g:

$$v_{02}(T,p) = v(T,0)\left[1 - 0.0894 \ln\left(1 + \frac{p}{B(T)}\right)\right] \quad (4)$$

with

$$v(T,0) = A_0 + A_1(T - 273.15) \quad (5)$$

and

$$B(T) = B_0 \exp[-B_1(T - 273.15)] \quad (6)$$

The temperature and pressure in eqs 2−6 are to be used in kelvin and pascal, respectively. In all calculations below the glass transition it turned out to have almost no effect on whether the experimental specific volume of the glassy polymer or the extrapolated value from the rubbery polymer (Tait equation) was used. Therefore, all specific polymer volumes throughout this work were calculated using the Tait equation (4).

All parameters used in those calculations are listed in Table 1.

To model the VLE behavior of the toluene−PS system, the simple Flory−Huggins equation was chosen.[49] The Poynting correction $\Pi_{01}^{LV} = 1$ and the ratio of the fugacity coefficients $\varphi_i^V/\varphi_{0i}^{LV} = 1$ were neglected. The resulting phase-equilibrium equation is

$$p = p_{01}^{LV}\phi_1 \exp\{(1-\phi_1) + \chi(1-\phi_1)^2\} \quad (7)$$

Table 1. Parameters for the Calculation of T_g and the Specific Volumes v_{01} and v_{02}

T_g parameters eq 1	v_{01} parameters[46] eq 3	v_{02} parameters[47] eqs 4−6
$T_{g1} = -156.15$ °C[47]	$A = 0.88257$	$A_0 = 0.9287$ cm^3/g
$T_{g2} = 105$ °C (DSC)	$B = 0.27108$	$A_1 = 5.131 \times 10^{-4}$ cm^3/(g K)
$\alpha_S = 0.001067$ 1/K[48]	$C = 591.79$	$B_0 = 216.9$ MPa
	$D = 0.29889$	$B_1 = 3.319 \times 10^{-3}$ 1/K
	$M_1 = 92.14$ g/mol	

Table 2. Parameters for Toluene−PS Used for the Modeling of the Isotherms (Figures 3 and 4)

T [°C]	χ parameter	p_{01}^{LV} [mbar]
30	0.296	48.7
70	0.291	270.8
80	0.294	387.1
110	0.243	992.2
115	0.267	1141.9

The calculations were performed using a constant interaction parameter χ. The results represent the experimental pressures in Figure 3 within an average relative error of 0.18%. The parameters used for the calculations are listed in Table 2.

In contrast to the isotherms for 110, 80, and 70 °C, the shape of the sorption isotherm changes when the temperature is decreased to 30 °C (Figure 4).

The first two points of the isotherm in Figure 4 lie below the calculated data using the Flory−Huggins model. They indicate a slight S-shaped form of the sorption isotherm showing an initial convex curvature of the isotherm toward the weight-fraction axis. This convex curvature of an isotherm is well-known from gas solubilities in glassy polymers[1] and is mostly explained using the dual-mode sorption model. According to this theory, the initial convex part of the isotherm is due to a Langmuir-type adsorption of gas molecules in small microvoids, trapped in the rigid glassy structure of the polymer. But neither the dual-mode sorption model nor the simple Flory−Huggins equation is capable of describing an S-shaped sorption isotherm, as is shown in Figure 4. The dual-mode sorption model only captures the initial convex form of the isotherm. This is due to the fact that the assumption of a linear Henry absorption is violated at higher concentrations. On the other hand, the simple Flory−Huggins model is not able to predict the convex form at low concentrations, but it captures the part at higher concentrations (rubbery polymer) correctly.

Therefore, in recent years considerable effort has been made to develop models to describe solubilities of gases and vapors in glassy polymers.[57−59,62] For example, the NELF model of Doghieri and Sarti[59] takes into account the nonequilibrium structure of the glass using the partial polymer density as an order parameter. Through

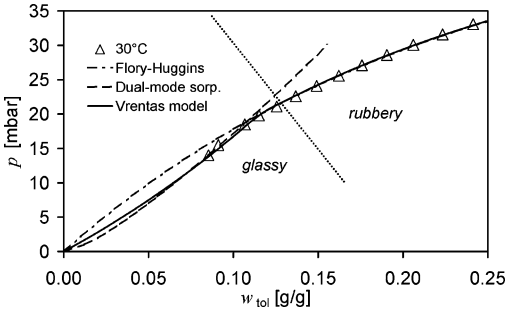

Figure 4. Experimental VLE data (vapor pressure as a function of solvent weight fraction) for toluene−PS at 30 °C.

Table 3. Additional Parameters Used for the Modeling of the 30 °C Isotherm for Toluene−PS with the Vrentas Model (Figure 4)

parameter	value
M_1	92.14 g/mol
$c_p - c_{pg}$	0.107 J/(g K)
A	650 K

an appropriate kinetic evolution of this parameter, they are able to describe solubilities in glassy polymers, e.g., the initial convex curvature of the isotherm for CO_2−polycarbonate.

Another model was developed by Vrentas et al.[62] Like Doghieri et al., they assume a continuous change in the structure of the polymer from a nonequilibrium configuration of the dry polymer to the equilibrium liquid structure at the concentration of the glass transition of the mixture. This is represented in the model by means of a concentration-dependent specific Gibbs free energy of the nonequilibrium polymer glass. Using the Flory−Huggins expression for the Gibbs free energy of mixing, they arrive at a phase equilibrium equation similar to eq 7:

$$p = p_{01}^{LV}\phi_1 \exp\{(1-\phi_1) + \chi(1-\phi_1)^2\}e^F \qquad (8)$$

with

$$F = \frac{M_1 w_2^{\,2}(c_p + c_{pg})A}{RT}\left(\frac{T}{T_g} - 1\right) \quad \text{for } T < T_g$$
$$F = 0 \quad \text{for } T \geq T_g \qquad (9)$$

Here M_1 is the molar mass of the solvent, and $c_p - c_{pg}$ is the difference of the specific isobaric molar heat capacities of the melt and the glass, respectively. The parameter A originates from the assumption of a linear decrease of the glass-transition temperature of the mixture with solvent concentration:

$$T_g = T_{g2} - Aw_1 \qquad (10)$$

From Figure 4 it can be seen that a proper description of the measured isotherm at 30 °C is possible using the parameters listed in Table 3. The difference of the isobaric heat capacities was set to 40% of the experimental value in order to fit the isotherm data. Otherwise, the calculated isotherm would have shown an even more pronounced S-shaped form.

All measured VLE data of the system toluene−polystyrene are listed in Table 4.

Diffusion. Figure 5 shows the sorption curves of the interval sorption measurements of toluene in a PS film of 100 μm thickness at 110 °C. Here W, the solvent mass relative to the dry polymer mass, is plotted vs the square root of the experimental time. Each sorption step is starting at the final mass uptake of the previous step and the experimental time $t = 0$.

All curves exhibit a linear initial slope until they bend to the equilibrium mass uptake. This behavior is one key criterion for Fickian diffusion.[36] Because the change in mass uptake in every sorption step is not more than $\Delta W = 0.01$, it should be possible to deduct a mean diffusion coefficient from each curve.[50]

For this purpose each sorption curve is plotted as $m(t)/m_\infty$ over $t^{1/2}$ as shown again for the 150−200 mbar step in Figure 6. $m(t)$ is the actual mass uptake in this step at time t, and m_∞ is the final mass uptake in this sorption step.

Crank[51] solved Fick's second law of diffusion for a constant diffusion coefficient for a free-standing film of

Table 4. Experimental VLE Data for Toluene−PS

T [°C]	w [g_{tol}/g_{total}][a]	p [mbar]	T [°C]	w [g_{tol}/g_{total}][b]	p [mbar]
30	0	0	110	0	0.0
	0.0853	14		0.0104	50.0
	0.0911	15.5		0.0220	100.0
	0.1068	18.5		0.0290	125.0
	0.1151	19.8		0.0355	149.9
	0.1256	21.1		0.0492	199.9
	0.1368	22.6		0.0640	249.9
	0.1491	24.1		0.0794	299.8
	0.1622	25.6		0.0954	350.0
	0.1759	27.1		0.1128	400.0
	0.1905	28.6		0.1312	449.8
	0.2061	30.1		0.1522	500.0
	0.2234	31.6		0.1748	550.0
	0.2414	33.1		0.1996	600.1
				0.2275	650.0
70	0	0		0.2595	700.1
	0.0215	25.0			
	0.0443	50.0	115	0	0
	0.0700	75.0		0.0039	20.0
	0.0993	100.0		0.0096	49.8
	0.1327	125.0		0.0200	99.9
				0.0305	150.0
80	0	0			
	0.0298	49.9			
	0.0642	100.0			
	0.1043	149.8			

[a] The uncertainty in the solvent weight fraction w calculated from error propagation for the toluene−PS measurements at 30, 70, and 80 °C is $\Delta w = \pm 0.001$, $\Delta w = \pm 0.0007$, and $\Delta w = \pm 0.0006$, respectively. [b] The uncertainty in the solvent weight fraction w calculated from error propagation for the toluene−PS measurements at 110 and 115 °C is $\Delta w = \pm 0.002$ and $\Delta w = \pm 0.0008$, respectively.

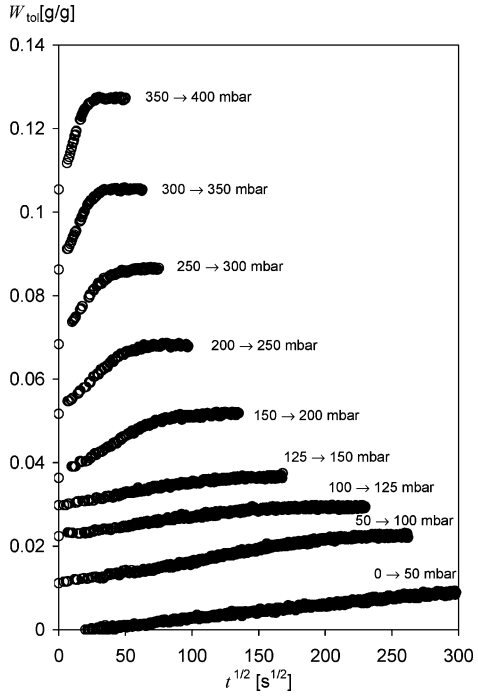

Figure 5. Experimental interval sorption curves for toluene−PS at 110°C; pressure steps up to 400 mbar.

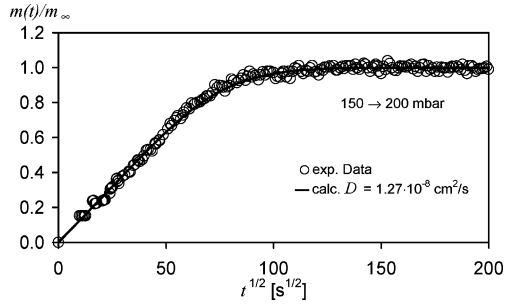

Figure 6. Experimental interval sorption curve and calculation (eq 8) for toluene−PS at 110 °C.

film thickness d which is exposed to sudden increase of the surface concentration on both sides.

$$\frac{m(t)}{m_\infty} = 1 - \sum_{n=0}^{\infty} \frac{8}{(2n+1)^2\pi^2} \exp\left\{-\frac{D(2n+1)^2\pi^2 t}{d^2}\right\} \tag{11}$$

In this equation d is the film thickness at the beginning of this sorption step and D is the mean diffusion coefficient. If the film is exposed to a higher surface concentration only from one side, like the 110 °C experiments in this work, eq 11 still holds, if twice the film thickness d is used.

Assuming the film thickness d is constant for each individual sorption interval, the mean diffusion coefficient D can be fitted to each experimental sorption curve.

For each sorption step, a new film thickness d is calculated using the volume fraction ϕ_1 of dissolved solvent from the preceding step, following eq 12.

$$d = \frac{d_0}{\sqrt[3]{1-\phi_1}} \tag{12}$$

This equation was derived under the assumption of no excess volume ($v^E = 0$) and isotropic three-dimensional swelling. The volume fraction ϕ_1 is easily calculated from the solvent weight fraction w_1 using eq 2. The modeling results using eq 11 for the step from 150 to 200 mbar are shown in Figure 6 as well.

Doing this for each individual sorption step, one ends up with a mean diffusion coefficient D for every weight fraction interval. To assign the diffusion coefficient to a specific weight fraction, the method of Vrentas et al.[50] is used. For an increasing diffusion coefficient which does not increase more than a factor of 20 in one sorption step, they propose to use the following assignment:

$$w_1 = w_{1,\text{start}} + 0.7(w_{1,\text{end}} - w_{1,\text{start}}) \tag{13}$$

For a decreasing diffusion coefficient the assignment is

$$w_1 = w_{1,\text{start}} + 0.56(w_{1,\text{end}} - w_{1,\text{start}}) \tag{14}$$

This procedure promises to make less than 5% error in the assignment for the given conditions. Figure 7 shows the semilogarithmic plot of the diffusion coefficient vs the solvent weight fraction at 110 °C. The diffusion coefficients for 80, 70, and 30 °C in Figure 7 are fitted to sorption curves at the respective temperature which exhibited Fickian diffusion behavior using the same procedure as described before.

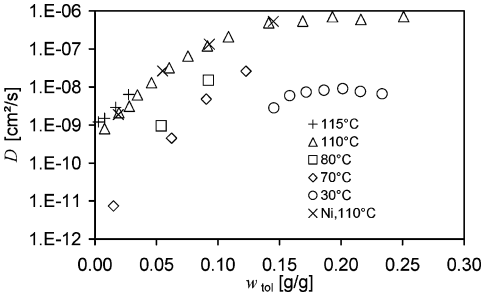

Figure 7. Diffusion coefficients for toluene in PS at 115, 110, 80, 70, and 30 °C as a function of toluene weight fraction (calculated for regions where Fickian diffusion was observed).

Table 5. Calculated Fickian Diffusion Coefficients for Toluene−PS

T [°C]	w [g_{tol}/g_{total}]	D [cm²/s] × 10^{-8}	T [°C]	w [g_{tol}/g_{total}]	D [cm²/s] × 10^{-8}
30	0.1454	0.28	110	0.0079	0.08
	0.1582	0.59		0.0195	0.21
	0.1717	0.73		0.0279	0.31
	0.1861	0.82		0.0346	0.62
	0.2015	0.90		0.0460	1.3
	0.2158	0.76		0.0604	3.2
	0.2335	0.66		0.0756	6.5
				0.0914	12
70	0.0150	0.00074		0.1085	21
	0.0623	0.045		0.1413	49
	0.0905	0.48		0.1689	54
	0.1227	2.6		0.1930	70
				0.2161	60
80	0.0539	0.095		0.2508	71
	0.0923	1.5			
			115	0.0028	0.12
				0.0079	0.15
				0.0169	0.29
				0.0273	0.63

All experimental diffusion coefficients obtained in this work are listed in Table 5.

Comparison of our data with diffusion coefficients measured by Ni[44] shows good agreement. The scattering in the higher diffusion coefficient range around 10^{-6} cm²/s in our data is certainly due to the relatively fast sorption process in the sample film of 100 μm initial film thickness. Only a few data points could be collected until equilibrium had been reached at that concentration.

Below the glass transition a certain sequence of different sorption features for the interval sorption measurements from low to high concentrations is expected. For amorphous polymer−solvent systems this sequence of sorption curve shapes is[52,53]

sigmoid → pseudo-Fickian → two-stage → pseudo-Fickian → Fickian

Figure 8 shows the experimental sorption curves for the toluene−PS system at 70 °C for a film of 46 μm initial thickness. Here a transition from pseudo-Fickian → sigmoid → pseudo-Fickian → Fickian is observed. It can be assumed that the film thickness as well as the pressure steps was too large to observe the two-stage behavior, and therefore the sigmoid part of the second stage is dominating this second interval sorption step. Nonetheless, the first sigmoid part of the sequence is missing, too.

The sorption curves for the interval measurements at 30 °C with a film of 29 μm initial thickness show all of the expected features (Figures 9 and 10).

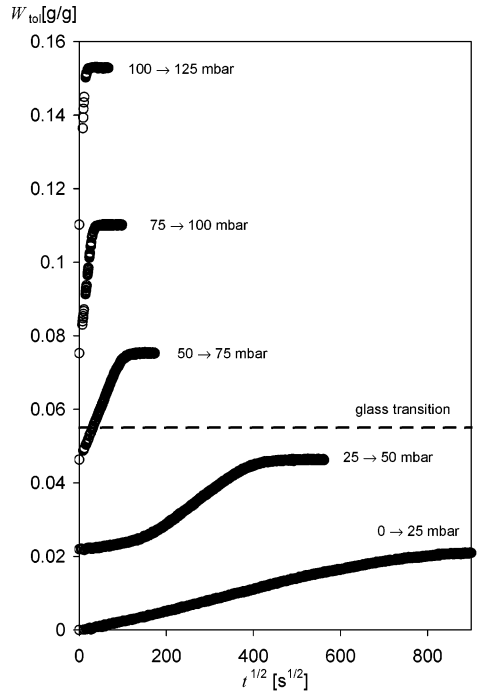

Figure 8. Experimental interval sorption curves for toluene−PS at 70 °C; glass transition calculated using eq 1.

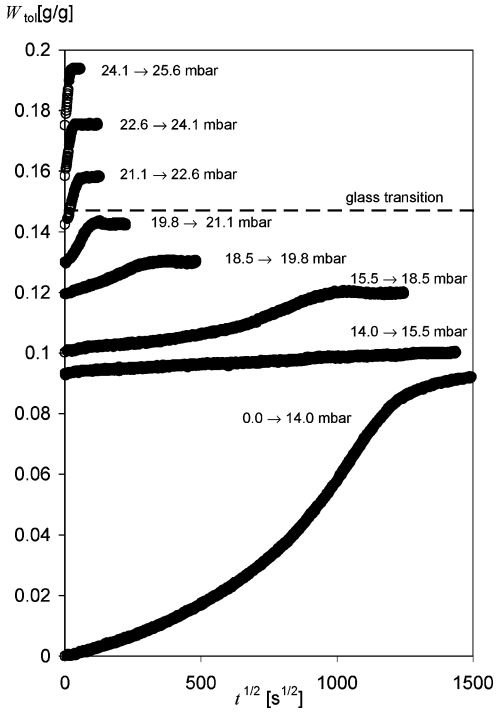

Figure 9. Experimental interval sorption curves for toluene−PS at 30 °C; steps up to 25.8 mbar; glass transition calculated using eq 1.

A first big sigmoid step (0−14 mbar) is followed by a more or less straight line (14−15.5 mbar, pseudo-Fickian). The next following four steps are separately displayed in Figure 10, where it is clearly seen that after a small initial linear part of the sorption curve a second sigmoid part concludes the sorption step from 15.5 to 18.5 mbar. This is well-known as two-stage sorption behavior. The next step (Figure 10b) looks almost Fickian, the second sigmoid part of the two-stage sorption curve having advanced to shorter times and more and more masking the initial linear part. The next two sorption curves (Figure 10c,d) have a slightly more visible S-shaped form than the preceding step, the latter exhibiting a very slow approach toward the equilibrium concentration. The step from 22.6 to 24.1 mbar is already of the Fickian type.

Those transitions between the different non-Fickian diffusion features are similar to the ones observed for benzene and ethylbenzene diffusing into amorphous polystyrene. Odani et al.[52] observed a direct transition from the two-stage sorption to Fickian sorption curves during benzene diffusion into polystyrene. Billovits et al.,[11] taking very small concentration intervals, showed that for ethylbenzene diffusing into polystyrene there is a range of slightly S-shaped sorption curves between in the transition from two-stage sorption to Fickian sorption curves.

The reason for non-Fickian diffusion behavior is generally assumed to be twofold:[36,53] On one hand, the characteristic relaxation time of the viscoelastic swelling of the polymer comes close to the characteristic diffusion time. This means that the swelling influences the mass transport, e.g., by changing the solubility or the diffusion coefficient with time. On the other hand, the concentration profiles lead to different swelling potentials across the film. To compensate for those, differential swelling stresses develop across the film; e.g., surface elements are compressed and inner elements are extended.

Both effects usually occur together, but there are certain conditions where the one or the other can be neglected.[53] In interval sorption measurements with small concentration changes at medium concentrations (two-stage and pseudo-Fickian features) in the sample the absence of differential swelling stresses is generally assumed. For example, the first Fickian uptake of the two-stage sorption can be explained by ordinary diffusion into an elastic swelling polymeric matrix until the matrix is more or less completely filled with solvent. In the second stage the polymer matrix relaxes or swells into its equilibrium configuration, slowly allowing additional solvent to enter the polymer until the final equilibrium is achieved. This has been shown experimentally by Long et al.[60]

If the polymer relaxation is the dominant feature for the sorption uptake, the characteristic relaxation time τ^* can be determined by $\tau^* = 2t^*$, where t^* is the time at the inflection point of the corresponding sorption curve.[69] Odani et al.[52,70] investigated the relaxation times of PS with ethyl acetate, methyl ethyl ketone (MEK), and benzene. They found a much steeper decrease of the characteristic relaxation time with concentration in amorphous PS compared to semicrystalline polymers. Concerning different solvents with similar molar volumes, they found the shorter relaxation times for the less soluble penetrant.

If the experimental results of this study are analyzed along the lines of Odani et al., it is found that the slope of t^* with initial concentration for the intermediate intervals from 15.5 to 21.1 mbar is approximately the one measured from Odani et al.[52] for an amorphous PS. As the solubility of toluene in PS lies between that of MEK and benzene, it is shown that time t^* is between that of MEK and benzene as well (Figure 11), which is in line with the findings of Odani et al. This is the case although the temperature in this study is 5 K higher than in Odani's investigation.

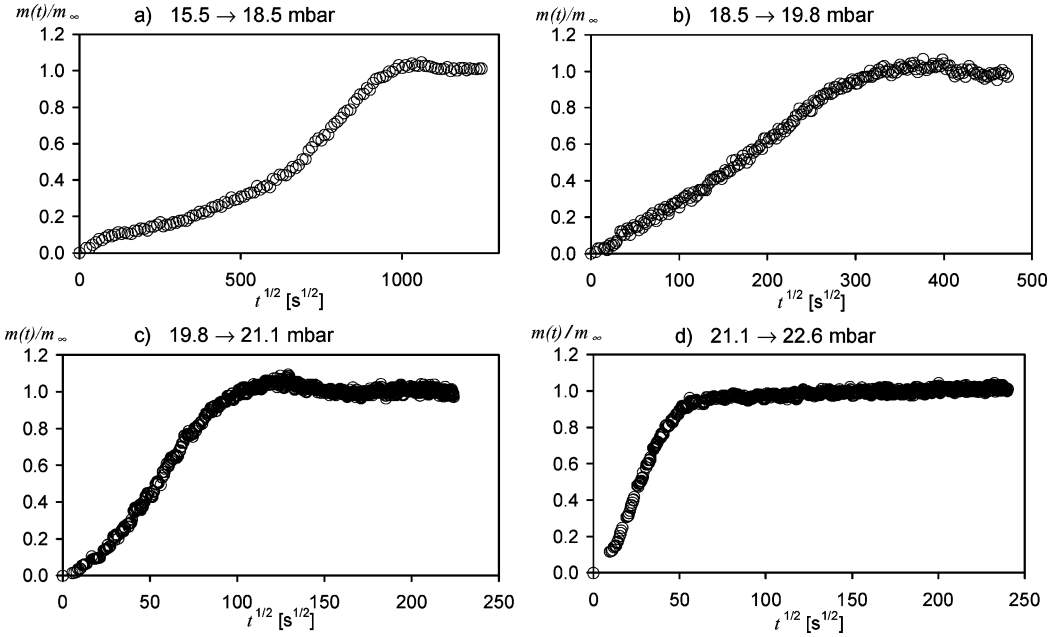

Figure 10. Experimental interval sorption curves for toluene−PS at 30 °C; steps from 15.5 to 22.6 mbar.

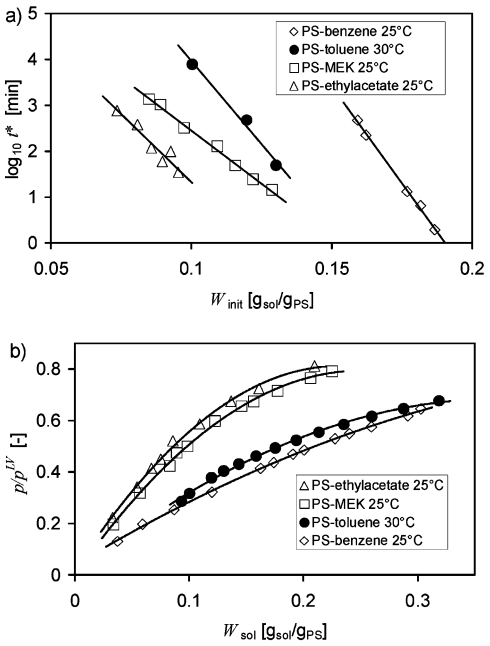

Figure 11. Comparison of sorption of different solvents in polystyrene; data from this work (filled symbols), data from Odani et al.[52] (open symbols). (a) Logarithmic correlation plot of t^* and initial solvent concentration W. (b) VLE data of the corresponding systems.

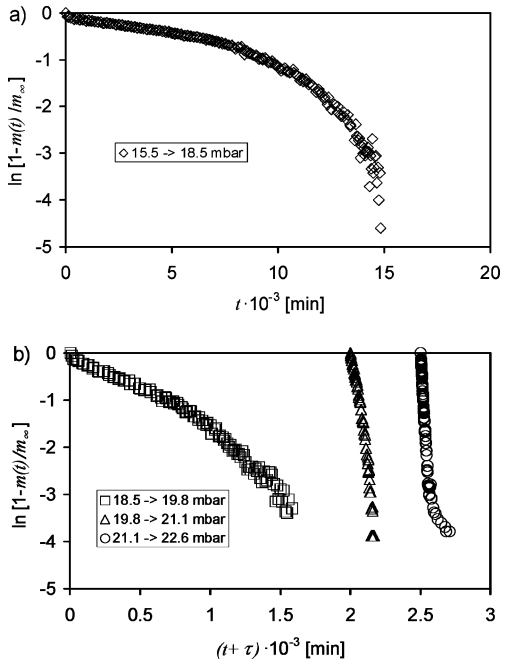

Figure 12. First-order kinetic analyses of the sorption curves: (a) pressure interval from 15.5 to 18.5 mbar; (b) pressure intervals from 18.5 to 22.6 mbar. The last two curves have been displaced along the time axis for clarity by $\tau = 2000$ min and $\tau = 2500$ min, respectively.

To judge whether an individual sorption step can be described with a single and constant relaxation time, the analysis of Petropoulos et al.[71] is applied. Plotting the four sorption curves from 15.5 to 22.6 mbar as $\ln(1 - m(t)/m_\infty)$ vs time t, the sorption curves exhibit first-order kinetics for short times (linear slope in Figure 12) but some deviation from this at long times.

The two-stage sorption step from 15.5 to 18.5 mbar shows a pronounced curvature toward the time axis at the end (Figure 12a). Following Petropoulos et al., those deviations are attributable to a marked concentration dependence of the corresponding relaxation time. This two-stage sorption step therefore cannot be described with a concentration-independent relaxation time due to the relatively large concentration interval used. The curvature of the two following sorption steps (Figure 12b) is almost negligible; thus, those curves should be properly described by a single constant relaxation time. The last sorption step in Figure 12b shows the opposite curvature toward the end. Petropoulos et al. showed that this behavior follows from a spectrum of relaxation times. The corresponding feature in the sorption curve (Figure 10d) is the slow creep toward the equilibrium concentration. This behavior was observed by Billovits et al. during their investigation of ethylbenzene sorption into PS, and they were later able to model the shape of this sorption curve by introducing a second constant relaxation time.[72]

Another interesting feature is the slight overshoot in the sorption curves for the intermediate pressure steps from 15.5 to 21.1 mbar. A similar behavior was previously observed in semicrystalline polymers[54] where solvent ingress into an amorphous polymer phase enhances the mobility of the polymer chains so that crystallization in the amorphous phase can take place. Because of this decrease of the amount of amorphous phase in the polymer, solvent molecules previously within this part of the polymer have to leave the polymer structure. Furthermore, Hong et al.[61] presented experimental evidence for overshoots due to a solvent induced order−disorder transition in a block copolymer system.

Baird et al.[56] observed overshoots also in the system *n*-pentane−polystyrene and attributed those to the development of small microvoids which formed in the unrelaxed glassy core ahead of the CASEII front.

Vrentas et al.[55] observed these overshoots in the system PEMA−ethylbenzene in the rubbery state and attributed this behavior to a temporarily oversaturated polymer, which is relaxing to its equilibrium conformation and therewith slowly rejects the solvent molecules. This is possibly due to the relatively slow relaxation of the PEMA chains compared to the diffusion of ethylbenzene into the film.

The overshoots in this study cannot be caused by solvent-induced crystallization because the polystyrene used here was an amorphous polystyrene, with a rather high molecular weight, which does not crystallize. Furthermore, there is no indication that the small pressure steps used in this work induced any crack or microvoid formation in the polymer structure. An explanation for the sorption overshoots observed in this work along the line of argument of Vrentas et al. seems the most reasonable although no final proof can be given at this point.

Conclusions

It was shown that reliable experimental results can be obtained with a new gravimetric sorption equipment. It is especially capable of performing the necessary long measurements in the glassy and the glass-transition region of polymer solvent systems.

For the system toluene−PS, VLE data were measured in the temperature range from 30 to 110 °C. The sorption isotherms above the glass transition exhibit the classical behavior, whereas far below the glass transition a slightly S-shaped sorption isotherm is found.

Above the glass transition, diffusion coefficients were determined from the mass uptake curves. Below the glass transition the sorption kinetics show pronounced anomalous or non-Fickian diffusion characteristics (sigmoid, two-stage). The concentration dependence of the characteristic relaxation time was found to be a steep function of solvent concentration. There is some indication of a second relaxation time being present at the transition to the Fickian diffusion regime. Sorption overshoots are found in a small range of experimental conditions.

Acknowledgment. The authors thank GE Bayer Silicones for supplying the PDMS.

References and Notes

(1) Vieth, W. R.; Sladek, K. J. *J. Colloid Sci.* **1965**, *20*, 1014.
(2) Koros, W. J.; Paul. D. R. *J. Polym. Sci., Polym. Phys. Ed.* **1976**, *14*, 1903.
(3) Stern, S. A.; Meringo, A. H. D. *J. Polym. Sci., Polym. Phys. Ed.* **1978**, *16*, 735.
(4) Sato, Y.; Yurugi, M.; Fujiwara, K.; Takishima, S.; Masuoka, H. *Fluid Phase Equilib.* **1996**, *125*, 129.
(5) Pfohl, O.; Riesesell, C.; Dohrn, R. *Fluid Phase Equilib.* **2002**, *202*, 289.
(6) Pawlisch, C. A.; Macris, A.; Laurence, R. L. *Macromolecules* **1987**, *20*, 1564.
(7) Pawlisch, C. A.; Bric, J. R.; Laurence, R. L. *Macromolecules* **1988**, *21*, 1685.
(8) Tihminlioglu, F.; Surana, R. K.; Danner, R. P.; Duda, J. L. *J. Polym. Sci., Part B: Polym. Phys.* **1997**, *35*, 1279.
(9) Fujita, H.; Kishimoto, A. *J. Polym. Sci.* **1958**, *28*, 547.
(10) Duda, J. L.; Kimmerly, G. K.; Sigelko, W. L.; Vrentas, J. S. *Ind. Eng. Chem. Fundam.* **1973**, *12*, 133.
(11) Billovits, G. F.; Durning, C. J. *Macromolecules* **1993**, *26*, 6927.
(12) Berens, A. R. *Polymer* **1977**, *18*, 697.
(13) Sanopoulou, M.; Roussis, P. P.; Petropoulos, J. H. *J. Polym. Sci., Part B: Polym. Phys.* **1995**, *33*, 993.
(14) Chen, W.-L.; Shull, K. R.; Papatheodorou, T.; Styrkas, D. A.; Keddie, J. L. *Macromolecules* **1999**, *32*, 136.
(15) Lösch, H. W.; Kleinrahm, R.; Wagner, W. In *Jahrbuch 1994 "Verfahrenstechnik und Chemieingenieurwesen"*; VDI-Verlagsgesellschaft Verfahrenstechnik und Chemieingenieurwesen (GVC); VDI-Verlag: Düsseldorf, 1994; p 117.
(16) Pfannschmidt, O.; Michaeli, W. In *Proceedings of the Annual Technical Conference of the Society of Plastics*; Atlanta, 1998; p 1918.
(17) Schnitzler, J. V.; Eggers, R. In *Supercritical Fluids—Materials and Natural Products Processing—Tome 1: Materials*; International Scociety for the Advancement of Supercritical Fluids: Nice, France, 1998; p 93.
(18) Treckmann, R. Ph.D. Thesis, Universität Kaiserslautern, Germany, 1999.
(19) Meares, P. *J. Am. Chem. Soc.* **1954**, *76*, 3415.
(20) Koros, W. J.; Paul, D. R. *J. Polym. Sci., Polym. Phys. Ed.* **1978**, *16*, 2171.
(21) Crank, J.; Park, G. C. In *Diffusion in Polymers*; Crank, J., Park, G. S., Eds.; Academic Press: London, 1968; p 4.
(22) Baschetti, M. G.; Piccinini, E.; Barbari, T. A.; Sarti, G. C. *Macromolecules* **2003**, *36*, 9574.
(23) Flichy, N. M. B.; Kazarian, S. G.; Lawrence, C. J.; Briscoe, B. J. *J. Phys. Chem. B* **2002**, *106*, 754.
(24) Chapman, B. R.; Gochanour, C. R.; Paulaitis, M. E. *Macromolecules* **1996**, *29*, 5635.
(25) Gall, T. P.; Lasky, R. C.; Kramer, E. J. *Polymer* **1990**, *31*, 1491.
(26) Nealey, P. F.; Cohen, R. E.; Argon, A. S. *Polymer* **1995**, *36*, 3687.
(27) Hyde, T. M.; Gladden, L. F. *Polymer* **1998**, *39*, 811.
(28) Long, F. A.; Thompson, L. J. *J. Polym. Sci.* **1955**, *15*, 413.
(29) Kishimoto, A.; Maekawa, E.; Fujita, H. *Bull. Chem. Soc. Jpn.* **1960**, *33*, 988.
(30) Vieth, W. R.; Howell, J. M.; Hsieh, J. H. *J. Membr. Sci.* **1976**, *1*, 177.
(31) Paul, D. R.; Koros, W. J. *J. Polym. Sci., Polym. Phys. Ed.* **1976**, *14*, 675.
(32) Horas, J. A.; Nieto, F. *J. Polym. Sci., Part B: Polym. Phys.* **1994**, *32*, 1889.
(33) Alfrey, T. *Chem. Eng. News* **1965**, *43*, 64.
(34) Vrentas, J. S.; Duda, J. L. *J. Polym. Sci., Polym. Phys. Ed.* **1977**, *15*, 441.
(35) Park, G. C. In *Diffusion in Polymers*; Crank, J., Park, G. S., Eds.; Academic Press: London, 1968; p 141.
(36) Fujita, H. *Fortschr. Hochpolym. Forsch.* **1961**, *3*, 1.
(37) Iwai, Y.; Kohno, M.; Akiyama, T.; Arai, Y. *Polym. Eng. Sci.* **1987**, *27*, 837.
(38) Iwai, Y.; Maruyama, S.; Fujimoto, M.; Miyamoto, S.; Arai, Y. *Polym. Eng. Sci.* **1989**, *29*, 773.
(39) Richman, D.; Long, F. A. *J. Am. Chem. Soc.* **1960**, *82*, 509.
(40) Stannett, V. In *Diffusion in Polymers*; Crank, J., Park, G. S., Eds.; Academic Press: London, 1968; p 41.
(41) Alentiev, A. Y.; Yampolski, Y. P. *J. Membr. Sci.* **2000**, *165*, 201.
(42) Kishimoto, A.; Fujita, H.; Odani, H.; Kurata, M.; Tamura, M. *J. Phys. Chem.* **1960**, *64*, 594.
(43) Odani, H.; Kida, S.; Kurata. M.; Tamura, M. *Bull. Chem. Soc. Jpn.* **1961**, *34*, 571.
(44) Ni, Y. C. Ph.D. Thesis, Pennsylvania State University, University Park, PA, 1978.
(45) Kelley, F. N.; Bueche, F. *J. Polym. Sci.* **1961**, *50*, 549.

(46) Daubert, T. E.; Danner, R. P. *Data Compilation Tables of Properties of Pure Compounds*; DIPPR-AICHE: New York, 1985.
(47) Danner, R. P.; High, M. S. *Handbook of Polymer Solution Thermodynamics*; DIPPR-AIChE: New York, 1993.
(48) Riddick, J. A.; Bunger, W. B.; Sakano, T. K. *Organic Solvents Physical Properties and Methods of Purification*, 4th ed.; Wiley-Interscience: New York, 1986.
(49) Flory, P. J. *Principles of Polymer Chemistry*; Cornell University Press: Ithaca, NY, 1953.
(50) Vrentas, J. S.; Duda, J. L.; Ni, Y. C. *J. Polym. Sci., Polym. Phys. Ed.* **1977**, *15*, 2039.
(51) Crank, J. *Mathematics of Diffusion*; Clarendon Press: London, 1967.
(52) Odani, H.; Hayashi, J.; Tamura, M. *Bull. Chem. Soc. Jpn.* **1961**, *34*, 817.
(53) Sanopoulou, M.; Petropoulos, J. *Macromolecules* **2001**, *34*, 1400.
(54) Durning, C. J.; Russel, W. R. *Polymer* **1985**, *26*, 131.
(55) Vrentas, J. S.; Duda, J. L.; Hou, A.-C. *J. Appl. Polym. Sci.* **1984**, *29*, 399.
(56) Baird, B. R.; Hopfenberg, H. B.; Stannett, V. T. *Polym. Eng. Sci.* **1971**, *11*, 274.
(57) Conforti, R. M.; Barbari, T. A.; Vimalchand, P.; Donohue, M. D. *Macromolecules* **1991**, *24*, 3388.
(58) Wissinger, R. G.; Paulaitis, M. E. *Ind. Eng. Chem. Res.* **1991**, *30*, 842.
(59) Doghieri, F.; Sarti, G. C. *Macromolecules* **1996**, *29*, 7885.
(60) Long, F. A.; Watt, I. *J. Polym. Sci.* **1956**, *21*, 554.
(61) Hong, S.-U.; Laurer, J. H.; Zielinski, J. M.; Samseth, J.; Smith, S. D.; Duda, J. L.; Spontak, R. J. *Macromolecules* **1998**, *31*, 2174.
(62) Vrentas, J. S.; Vrentas, C. M. *Macromolecules* **1991**, *24*, 2404.
(63) Baughan, E. C. *Trans. Faraday Soc.* **1948**, *44*, 495.
(64) Bawn, C. E. H.; Freeman, R. F. J.; Kamaliddin, A. R. *Trans. Faraday Soc.* **1950**, *46*, 677.
(65) Tsutsui, K.; Katsumata, T.; Yamamoto, Y.; Fukatsu, H.; Yoshimizu, H.; Kinoshita, T.; Tsujita, Y. *Polymer* **1999**, *40*, 3815.
(66) Katayama, T.; Matsumara, K.; Urahama, *Kogaku Kogaku* **1971**, *35*, 1012.
(67) Wang, K.; Chen, Y.; Fu, J.; Hu, Y. *Chin. J. Chem. Eng.* **1993**, *1*, 65.
(68) Wang, N.-H.; Takashima, S.; Masuoka, H. *Kagaku Kogaku Ronbunshu* **1989**, *15*, 795.
(69) Tamura, M.; Yamada, K.; Odani, H. *Rep. Prog. Polym. Phys. Jpn.* **1963**, *6*, 163.
(70) Odani, H.; Kida, S.; Tamura, M. *Bull. Chem. Soc. Jpn.* **1966**, *39*, 2378.
(71) Petropoulos, J. H.; Roussis, P. P. In *Permeability of Plastic Films and Coatings to Gases, Vapours and Liquids*; Hopfenberg, H. B., Ed.; Plenum: New York, 1974; p 219.
(72) Billovits, G. F.; Durning, C. J. *Macromolecules* **1994**, *27*, 7630.

MA050353O